Chemical Science

Accepted Manuscript

This article can be cited before page numbers have been issued, to do this please use: C. Mi, L. Ma, X. Wen, Y. Hou, X. Dao, A. Peng, Q. Shi and H. Huang, *Chem. Sci.*, 2026, DOI: 10.1039/D6SC01097K.

ROYAL SOCIETY OF CHEMISTRY

rsc.li/chemical-science

View Article Online
DOI: 10.1039/D6SC01097K

ARTICLE

Enhanced Visible-Light Photoredox Catalysis with Rubicene-Embedded Polycyclic Aromatic Hydrocarbons (PAHs)

Received 00th January 20xx,
Accepted 00th January 20xx

DOI: 10.1039/x0xx00000x

Chunchun Mi,[a†] Liangzhuo Ma,[a†] Xuan Wen,[a] Yuqi Hou,[a] Xuelin Dao,[a] Aidong Peng,[a] Qinqin Shi,*[a] and Hui Huang[b]

Visible-light-absorbing, metal-free photoredox catalysts are attractive because they are inexpensive and offer tunable redox potentials. However, the use of organic photocatalysts is often limited by their incompatibility with strongly acidic or basic media and by short excited-state lifetimes. Here we report a series of rubicene-based organic photoredox catalysts that operate under visible-light irradiation and promote substitution and addition reactions. Mechanistic studies, including radical-trapping experiments and Stern-Volmer fluorescence-quenching analyses, support a single-electron-transfer (SET) pathway. Notably, the rubicene-based catalysts exhibit excellent operational stability and higher reactivity than commercial metal-free photocatalysts, indicating a broad scope and high tolerance in metal-free photoredox transformations.

Introduction

Over the past decade, visible-light-absorbing, metal-free photoredox catalysis has emerged as a powerful platform for organic synthesis owing to its mild and excellent sustainable reaction conditions.[1] A variety of catalysts, including small molecular dyes[2] and polymeric organic semiconductors,[3] have been developed by virtue of suitable redox potentials and long-lived excited states ($\tau_f \geq 1$ ns). Among them, small molecular dyes have been extensively studied in a wide range of transformations, such as C(sp^3)-C(sp^2), C(sp^3)-C(sp^3), C(sp^2)-C(sp^2), C-Br, C-Cl, C-S, C-N and C-P bond-formation, as well as in alkene isomerization.[2a-d, 2f, 3a, 4] To function efficiently under visible light, such photocatalysts generally require both long-lived excited states and high chemical stability. For achieving extended excited-state lifetimes, most organic photoredox catalysts, including benzophenone, DDQ, acridinium and eosin Y (Figure 1A), rely on the sensitive auxochromes such as carbonyl, ester, amide, halogen, and carboxyl groups,[2c, 2d, 3a, 5] to enhance intersystem crossing ($\tau_T \geq 1$ μs) and tune their absorption profiles. However, carbonyl, ester and carboxyl groups are susceptible to degradation under strong ases (e.g., Grignard reagents, sodium hydroxide),[5-6] whereas amides are unstable under strongly acidic conditions (e.g., hydrochloric acid).[7] To simultaneously achieve visible-light absorption and excellent chemical robustness, donor-acceptor (D-A) type molecular dyads, such as 4CzPN, 4CzIPN, Th-BO-Th, and Th-BT-Th (Figure 1B), have been developed as efficient metal-free photoredox catalysts.[2a] Nevertheless, their narrow bandgaps tend to reduce radiative decay rates and shorten fluorescence lifetimes according to the energy-gap law.[8] Thus, there remains a clear need for the development of organic photocatalysts that combine long-lived excited states with high chemical stability under diverse reaction conditions.

Recently, Wang reported a rubicene null aggregates, exhibit ultrahigh triplet yield (192%).[9] Shi and co-workers reported a series of chalcogen-doped rubicene polycyclic aromatic hydrocarbons (PAHs) that exhibit high intersystem-crossing quantum yields (ϕ_{ISC} up to 90%), strong absorption in the visible region (400-550 nm) and tunable photoredox potentials (Figure 1C).[10] Importantly, the exceptionally chemically and thermally stable PAHs frameworks are expected to tolerate harsh reaction conditions and thereby offer broad synthetic utility. Motivated by these features, we hypothesized that rubicene scaffolds could serve as promising platforms for photocatalytic reactions. Here we develop a family of rubicene-based photocatalysts that support a broad range of visible-light-driven transformations, including trifluoromethylation, heteroarylation, borylation, thioetherification and hydromethylthiolation (Figure 1C). Notably, these catalysts display superior efficacy and excellent tolerance under acidic and basic conditions, at elevated temperatures and in common organic solvents, highlighting the robustness of the catalytic system. In addition, radical-trapping experiments and Stern-Volmer fluorescence-quenching analyses support a single-electron-transfer (SET) process.

Results and Discussion

Reaction conditions optimization

[a] College of Materials Science and Opto-Electronic Technology, University of Chinese Academy of Sciences, Beijing 100049 E-mail: shiqinqin@ucas.ac.cn
[b] School of Chemical Engineering and Technology, State Key Laboratory of Chemical Engineering and Low-Carbon Technology, Tianjin University, Tianjin 300072
† These authors contributed equally to this work.
Supplementary Information available: [details of any supplementary information available should be included here]. See DOI: xxxxxx

View Article Online
DOI: 10.1039/D6SC01097K

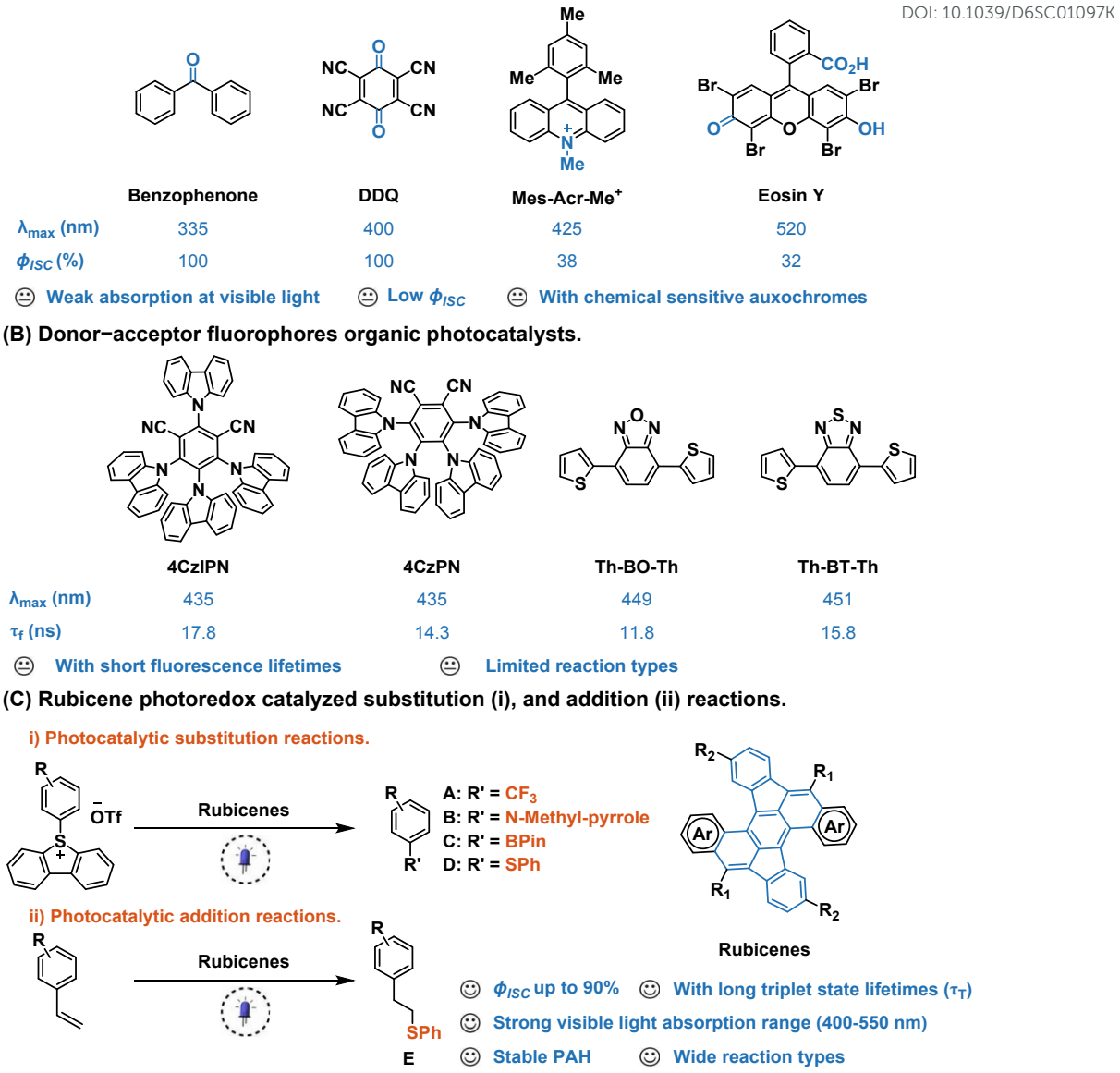

Figure 1. (**A**) Traditional organic photocatalysts. (**B**) Donor–acceptor fluorophores organic photocatalysts. (**C**) Rubicene photoredox catalyzed substitution (i), and addition (ii) reactions.

Considering the advantages of biphenylsulfonium salts, such as high selectivity, high reduction potential, and easy accessibility,[11] they were selected as nucleophiles in the challenging trifluoromethylation reaction. Trifluoromethyl groups in drug molecules are associated with enhanced blood-brain barrier penetration,[12] increased metabolic stability and improved selectivity.[13] Thus, we first examined the photocatalytic trifluoromethylation of a biphenylsulfonium salt (Table 1). The reaction was carried out using [$CuCF_3$], generated from CuSCN, CsF and $TMSCF_3$ as the trifluoromethylating reagent in-situ, with rubicene as the photoredox catalyst in acetone:DMF (8:1) under 467 nm irradiation at room temperature for 13 h. Under these conditions, 4-(trifluoromethyl)-1,1′-biphenyl (**A1**) was obtained in 61% yield (entry 1). In view of the relatively low ϕ_{ISC} of rubicene (Figure 3A), we next screened rubicene derivatives with higher ϕ_{ISC} values, including Ben-rubicene, O-rubicene, S-rubicene and Se-rubicene (entries 2-5). Notably, use of S-rubicene afforded **A1** in 87% yield (entry 4). As expected, no product was detected when the reaction was conducted in the absence of a photocatalyst or in the dark (entries 6-7). To exclude any contribution from trace transition metals, sublimed S-rubicene was evaluated (entry 8) to generate **A1** in 84% yield, indicating that the effect of trace metal impurities is negligible.

Mechanistic investigations

To elucidate the role of the rubicene photocatalysts, we performed a series of mechanistic studies. The addition of 2,2,6,6-(tetramethylpiperidin-1-yl)oxyl (TEMPO) or 2,6-di-tert-butyl-4-methylphenol (BHT) resulted in formation of **A1** in 74% and 65% yield, respectively (entries 1-2, Figure 2A), only slightly suppressing the photocatalytic reaction. This modest inhibition suggests that copper intermediates trap radicals more efficiently than the added radical scavengers.[14] To further probe the mechanism, Stern-Volmer fluorescence-quenching

View Article Online
DOI: 10.1039/D6SC01097K

Table 1. Optimization of the trifluoromethylation of biphenylsulfonium salts.

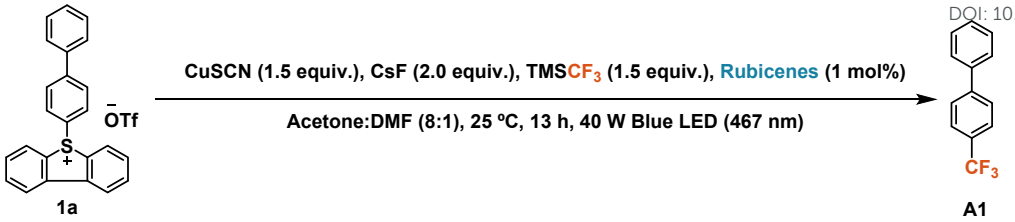

Entry	Photocatalysts	Yield (%)[a]
1	Rubicene	61
2	Ben-rubicene	53
3	O-rubicene	48
4	S-rubicene	87
5	Se-rubicene	80
6	-	0
7[b]	S-rubicene	0
8[c]	S-rubicene	84

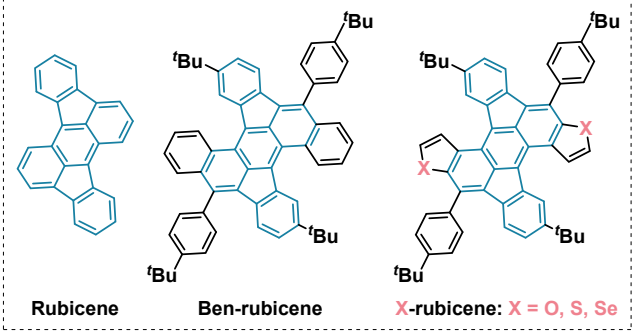

[a]Unless otherwise noted, a mixture of (a solution of CuSCN (0.15 mmol, 1.5 equiv.), CsF (0.2 mmol, 2.0 equiv.), and $TMSCF_3$ (0.15 mmol, 1.5 equiv.) in DMF (0.5 mL), biphenylsulfonium salts(1a) (0.10 mmol, 1.0 equiv.), rubicenes (1 mol%) in acetone (4.0 mL), irradiated with a blue LED (467 nm) lamp at 25 °C for 13h. Isolated yields was gaven; [b]In the darkness; [c]S-rubicene is purified by sublimation.

(A) Radical trapping experiment.

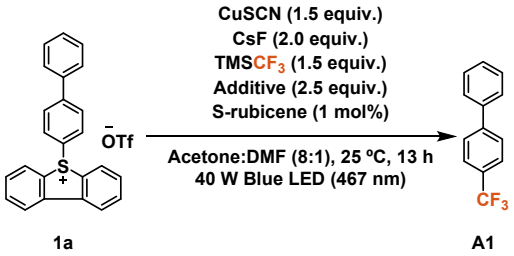

Entry	Additive (2.5 equiv.)	A1 Yield (%)
1	TEMPO	72
2	BHT	64

(B) Stern-Volmer fluorescence quenching experiments.

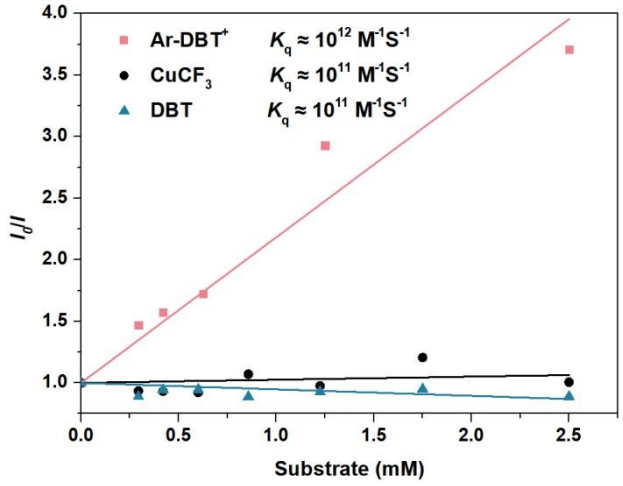

(C) Proposed mechanism.

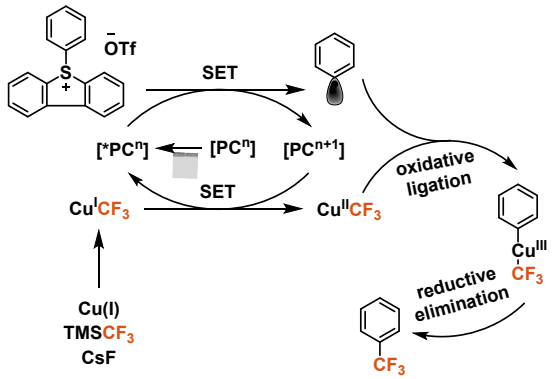

(D) Hammett-plot.

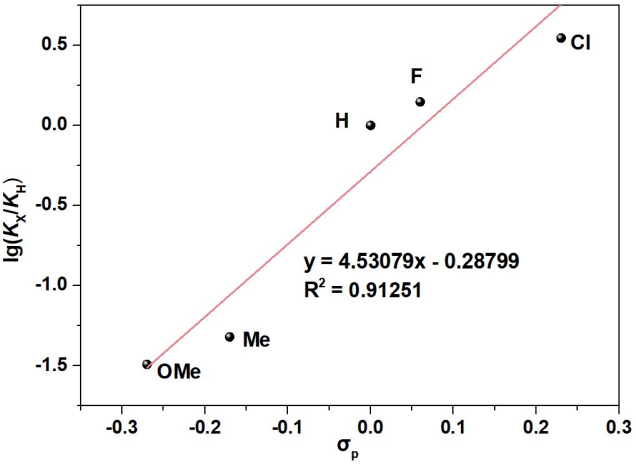

Figure 2. (**A**) The radical trapping experiments in the presence of various radical inhibitors. Conditions: a solution of CuSCN (0.15 mmol, 1.5 equiv.), CsF (0.2 mmol, 2.0 equiv.), and $TMSCF_3$ (0.15 mmol, 1.5 equiv.) in DMF (0.5 mL), **1a** (1.0 equiv.), S-rubicene (1

View Article Online
DOI: 10.1039/D6SC01997H

mol%), additive (2.5 equiv.), acetone (0.025 M), 25 °C, kessil 40W blue LED (467 nm), 13 h. (**B**) Stern-Volmer plot for S-rubicene in DMF/acetone (*v*/*v*: 1:1) (100 μM) with varying [$CuCF_3$], aryl sulfonium salt, dibenzothiophene (DBT). (**C**) Proposed mechanism of the S-rubicene photoredox catalyzed trifluoromethylation of biphenylsulfonium salts. (**D**) Hammett-plot.

experiments were carried out to assess electron transfer between S-rubicene and either [$CuCF_3$] or the aryl sulfonium salt (Supporting Information Figures S1 and S2). The emission of S-rubicene was efficiently quenched by aryl sulfonium salts, whereas dibenzothiophene (DBT) and [$CuCF_3$] induced only weak quenching (Figure 2B), indicating a SET process between S-rubicene and the aryl sulfonium salt. These observations are consistent with the radical-trapping experiments. Furthermore, we examined the relative rates of reactions involving aryl sulfonium salts bearing para-substituted benzene groups (MeO, Me, H, F and Cl; Figure 2D). The positive Hammett ρ value (+4.5) indicates that the reduction of electron density at the sulfonium salt reaction center in the presence of electron-withdrawing groups (EWGs) influences the kinetics of the photocatalytic mechanism. Specifically, EWGs are expected to further diminish the electron density at the reaction center, thereby facilitating electron transfer (ET) from the S-rubicene photocatalyst. Consequently, it is plausible that ET from the catalyst to the substrate is involved in the rate-determining step of the reaction. On the basis of these results, we propose the catalytic cycle shown in Figure 2C. First, the ground-state photocatalyst [PC^n] is excited by blue light to give [$*PC^n$]. This excited state undergoes SET with the aryl sulfonium salt to afford [PC^{n+1}] and the corresponding aryl radical. Then, the oxidized photocatalyst [PC^{n+1}] performs SET with [Cu^ICF_3], regenerating [PC^n] and forming [$Cu^{II}CF_3$], which captures the aryl radical to generate a $PhCu^{III}CF_3$ intermediate. Finally, reductive elimination from this intermediate furnishes the trifluoromethylated aryl product.

To gain further insight into the role of rubicene, we examined the triplet-state lifetimes (τ_T) of rubicene derivatives in chloroform solution by transient absorption spectroscopy using a tunable-wavelength nanosecond laser. The triplet lifetimes of rubicene, Ben-rubicene, O-rubicene, S-rubicene and Se-rubicene were determined to be 20.4, 19.5, 52.6, 30.3 and 13.1 μs, respectively, values that are consistent with high catalytic efficiency in photoredox processes. The fluorescence lifetimes range from 1.7 ns to 4.9 ns. Notably, since the photocatalysts exhibit fluorescence lifetimes greater than 1 ns, their singlet excited states may also participate in the photoinduced electron transfer (PET) process.[2f] Notably, the high intersystem-crossing quantum yields (ϕ_{ISC}) of these rubicenes, ranging from 23% to 90%, indicate that the T_1 excited state readily engages in bimolecular reactions with substrates and can efficiently mediate both energy transfer (EnT) and electron transfer (ET).[2f] In addition, the excited states of rubicenes display strong oxidizing ($E_{1/2}(^*P/P^-)$ = +0.79 to +1.75 V) and reducing ($E_{1/2}(P^+/^*P)$ = -1.58 to –2.34 V) abilities under visible-light excitation. These redox potentials are comparable to or exceed those of many metal complexes and organic dyes,[2a, 2f] suggesting broad substrate compatibility (Figure 3A). To

(A) Photoredox potentials, ϕ_{ISC} and τ_T of the rubicenes.

Compounds	λ_{max} (nm)	ϕ_{ISC} (%)	τ_T (μs)
rubicene	529	23	20.4
Ben-rubicene	413	44	19.5
O-rubicene	502	40	52.6
S-rubicene	500	78	30.3
Se-rubicene	513	90	13.1

(B) The ^{1}H-NMR spectra of rubicene after stirring at acid or base.

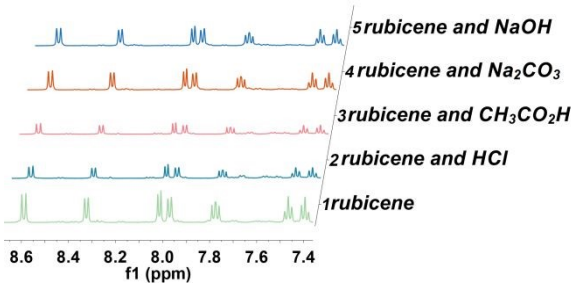

(C) The UV-vis absorption spectra of rubicene.

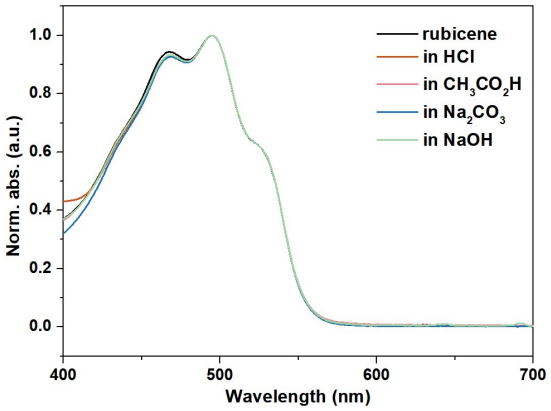

(D) The UV-vis absorption spectra of rubicene in common solvents.

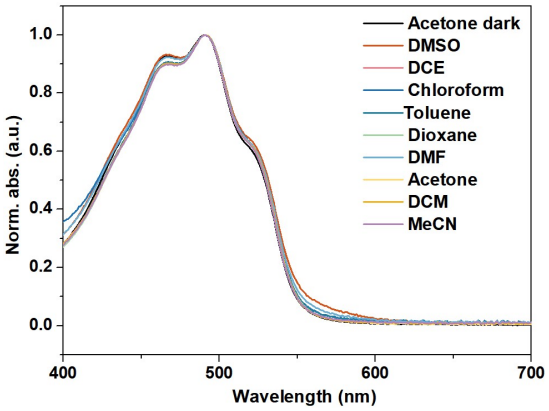

Figure 3. (**A**) Local absorbance maximum, ϕ_{ISC} and τ_T of the rubicenes: rubicene, Ben-rubicene, O-rubicene, S-rubicene, Se-rubicene. (**B**) ^{1}H-NMR spectra of rubicene after stirring at acid or base (0.25 M) in acetone for 6 h. (**C**) The UV-vis absorption spectra of rubicene after stirring at acid or base (0.25 M) in acetone for 6 h. (**D**) The UV-vis absorption spectra of rubicene solution after blue light irradiation.

View Article Online
DOI: 10.1039/D6SC01097K

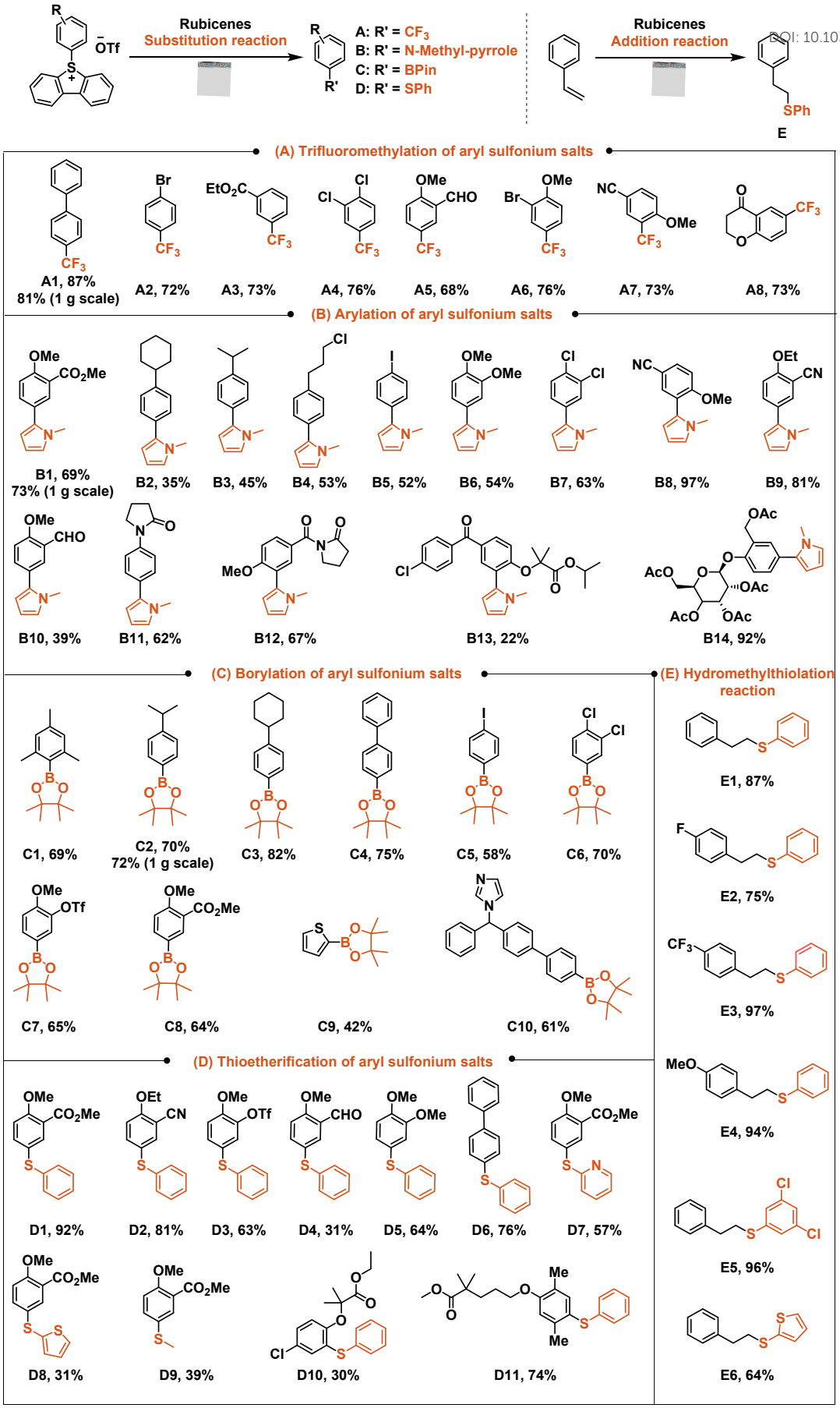

Figure 4. The substrate scope. (**A**) Trifluoromethylation of aryl sulfonium salts. Reaction conditions: (CuSCN (1.5 equiv.), CsF (2.0

View Article Online
DOI: 10.1039/D6SC01097K

equiv.), $TMSCF_3$ (1.5 equiv.) in DMF (0.3 M) for 30 min.), aryl sulfonium salts (1.0 equiv.), S-rubicene (1 mol%), acetone (0.025 M), kessil 40W blue LED (467 nm) lamp, 25 °C, N_2, 12 h. (**B**) Arylation of aryl sulfonium salts. Reaction conditions: Aryl sulfonium salts (1.0 equiv.), N-Methyl pyrrole (20.0 equiv.), S-rubicene (1 mol%), KOAc (5.0 equiv.), DMSO (0.2 M), kessil 40W blue LED (440 nm) lamp, 25 ℃, N_2, 35 h. (**C**) Borylation of aryl sulfonium salts. Reaction conditions: Aryl sulfonium salts (1.0 equiv.), B_2Pin_2 (5.0 equiv.), rubicene (2 mol%), pyridine (5.0 equiv.), acetone (0.25 M), kessil 40W blue LED (427 nm) lamp, 25 ℃, N_2, 35 h. (**D**) Thioetherification of aryl sulfonium salts. Reaction conditions: Aryl sulfonium salts (1.0 equiv.), RSSR (5.0 equiv.), S-rubicene (2 mol%), pyridine (5.0 equiv.), acetone (0.5 M), kessil 40W blue LED (440 nm) lamp, 25 ℃, N_2, 25 h. (**E**) Hydromethylthiolation reaction. Reaction conditions: Styrene (1.0 equiv.), RSSR (5.0 equiv.), Se-rubicene (1 mol%), 2,6-dimethyl-1,4-dihydro-pyridine-3,5-dicarboxylic acid di-tert-butyl ester (Hantzsch ester) (2.0 equiv.), MeCN (0.1 M), kessil 40W blue LED (440) lamp, 25 ℃, N_2, 25 h. Isolated yields shown.

assess the chemical stability of rubicenes, 1 mol% of rubicene was stirred in strongly acidic or basic media for 6 h. The ^{1}H-NMR and UV-vis absorption spectra showed negligible changes (Figures 3B and 3C). It is worth pointing out that, the absorption spectra recorded before and after treatment showed no decrease in intensity (Figures S4), further indicating excellent chemical robustness. Furthermore, rubicene solutions were irradiated with blue light for 6 h in common organic solvents including DMSO, DCE and chloroform (Figure 3D). The UV-vis spectra remained essentially unchanged, demonstrating that rubicenes are photostable under visible-light irradiation in a range of solvents.

Substrate scope

With optimized reaction conditions in hand, we next examined the trifluoromethylation of various substrates (Figure 4A). Phenylsulfonium salts bearing halogen (**A2**, **A4**, **A6**), ester (**A3**), aldehyde (**A5**), alkoxy (**A5**, **A6**, **A7**), cyano (**A7**) and carbonyl (**A8**) substituents were well tolerated, affording the desired products in ≥68% yield**.** Notably, para-bromo-, 3,4-dichloro- and 3-bromo-4-methoxy-substituted benzene sulfonium salts gave the corresponding trifluoromethylated products **A2**, **A4** and **A6** in 72%, 76% and 76% yields, respectively, providing useful handles for further derivatization. To demonstrate the versatility of the rubicene-based photoredox catalyst, we next investigated a series of additional transformations (Figures 4B to 4E). N-methylpyrroles are key motifs in many biomolecules, pharmaceuticals,[15] and conducting copolymers.[16] The optimized conditions (Supporting Information Table S2) were compatible with halogen (**B4**, **B5**, **B7**, **B13**), ester (**B1**, **B13**), aldehyde (**B10**), alkoxy (**B1**, **B6**, **B8**, **B9**, **B10**, **B12**, **B13**, **B14**), cyano (**B8**, **B9**) and amide (**B11**, **B12**) substituents on phenylsulfonium salts, delivering thedesired products in 22-97% yield. Late-stage functionalization of bioactive molecules **B13** and **B14** furnished the corresponding products in 22% and 92% yield, respectively, illustrating that the photocatalytic protocol can be applied to structurally complex substrates. Organoboron compounds, valued for their low toxicity, mild reaction conditions and broad synthetic utility,[17] have attracted considerable attention. Here we report a transition-metal-free borylation of aryl sulfonium salts using rubicene as a photoredox catalyst (Figure 4C, **C1**-**C10**). Para-iodo-, 3,4-dichloro- and 3-trifluoromethanesulfonate-substituted benzene sulfonium salts afforded the corresponding borylated products **C5**, **C6** and **C7** in 58%, 70% and 65% yield, respectively, again providing opportunities for further downstream derivatization. We then explored thioetherification (Figure 4D), a widely used transformation in synthetic chemistry.[18] Phenylsulfonium salts bearing ester (**D1**, **D7**, **D8**-**D11**), cyano (**D2**), trifluoromethanesulfonate (**D3**), aldehyde (**D4**), halogen (**D10**) and alkoxy (**D1**-**D5**, **D7**-**D11**) groups were well tolerated, affording thioether products in 30-92% yield. The method was also suitable for the synthesis of heteroaromatic thioethers (**D7**, **D8**) and an alkyl thioether (**D9**), which were obtained in 57%, 31% and 39% yield, respectively. More importantly, late-stage functionalization of bioactive molecules was likewise achieved, affording thioether products **D10** and **D11** in 30% and 74% yield, respectively. Furthermore, we demonstrated the applicability of this platform to hydromethylthiolation using styrenes as substrates (Figure 4E). The reaction tolerated halogen (**E2**, **E3**, **E5**) and alkoxy (**E4**) substituents, delivering the corresponding products in 75-97% yield. The method also enabled the synthesis of a heteroaromatic thioether (**E6**) in 64% yield. Finally, gram-scale reactions were conducted to obtain products **A1**, **B1** and **C2**. Under optimal conditions with slightly longer reaction times, products **A1**, **B1** and **C2** were obtained in 81%, 73% and 72% yields, respectively (Figure 4), which are comparable to the yields (87%, 69% and 70%) achieved under small-scale conditions.

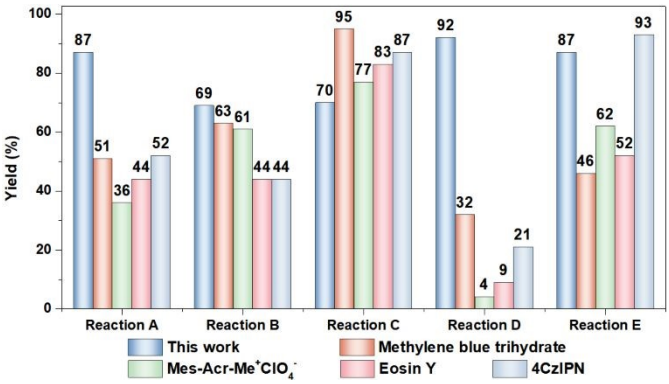

Figure 5. Comparison between the rubicenes organic catalysts and other organic catalysts. Isolated yields were given.

We next benchmarked the catalytic performance of the rubicene-based photocatalyst against commercial organic photocatalysts in the A, B, C, D and E reactions (Figure 5). The results show that in reaction D, using S-rubicene as the photocatalyst afforded the desired product in 92% yield, whereas the yields with commercial photocatalysts were all below 32%. Similarly, in reaction A, S-rubicene gave the desired product in 87% yield, while the yields with commercial photocatalysts were all below 51%. Furthermore, across all five reactions (A-E), the rubicene-based photocatalysts consistently

exhibited high catalytic efficiency, whereas the commercial photocatalysts showed high efficiency only in selected reactions. Together, these comparisons indicate that rubicene-based photocatalysts offer a robust and versatile choice for synthetic applications.

Conclusions

In summary, we have developed a class of rubicene-based photocatalysts that enable highly efficient photoredox transformations, including trifluoromethylation, heteroarylation, borylation, thioetherification of aryl sulfonium salts, and hydromethylthiolation. These reactions proceed under visible light and benefit from the exceptional chemical stability, strong oxidizing and reducing abilities, long excited-state lifetimes and high triplet quantum yields of the rubicene scaffolds. The methods show broad substrate scope and high functional-group tolerance, and are applicable to the late-stage modification of structurally complex, bioactive molecules. Radical-trapping experiments and Stern-Volmer fluorescence-quenching analyses support a SET mechanism. The combination of robustness, tunable redox properties and long-lived excited states positions rubicene as promising photocatalysts for scalable and more sustainable chemical manufacturing.

Author contributions

Q.S. conceived the idea and supervised the projects. C.M. conducted the research. C.M., L.M. and X.W. performed the experiments. Y.H. performed the spectroscopic tests. C.M., H.H., A.P. and Q.S. wrote the manuscript.

Conflicts of interest

There is no conflict of interest to report.

Data availability

All data needed to evaluate the conclusions in the paper are present in the paper and/or the Supplementary Materials.

Acknowledgements

The authors acknowledge the financial support from the NSFC (52222309 (Q.S.)), the Strategic Priority Research Program of Chinese Academy of Sciences (XDB 0520103), National Key R&D Program of China (Nos. 2024YFB3614300), Xiaomi Young Talents Program, and Fundamental Research Funds for the Central University.

Notes and references

1. (a) E. B. Corcoran, M. T. Pirnot, S. Lin, S. D. Dreher, D. A. DiRocco, I. W. Davies, S. L. Buchwald and D. W. C. MacMillan, *Science* 2016, **353**, 279-283; (b) P. Bellotti, H.-M. Huang, T. Faber and F. Glorius, *Chem. Rev.* 2023, **123**, 4237-4352.
2. (a) J. Luo and J. Zhang, *ACS Catal.* 2016, **6**, 873-877; (b) I. Ghosh, T. Ghosh, J. I. Bardagi and B. König, *Science* 2014, **346**, 725-728; (c) A. Joshi-Pangu, F. Lévesque, H. G. Roth, S. F. Oliver, L.-C. Campeau, D. Nicewicz and D. A. DiRocco, *J. Org. Chem.* 2016, **81**, 7244-7249; (d) N. A. Romero, K. A. Margrey, N. E. Tay and D. A. Nicewicz, *Science* 2015, **349**, 1326-1330; (e) W. Zhang, X.-X. Xiang, J. Chen, C. Yang, Y.-L. Pan, J.-P. Cheng, Q. Meng and X. Li, *Nat. Commun.* 2020, **11**, 638; (f) N. A. Romero and D. A. Nicewicz, *Chem. Rev.* 2016, **116**, 10075-10166.
3. (a) I. Ghosh, J. Khamrai, A. Savateev, N. Shlapakov, M. Antonietti and B. König, *Science* 2019, **365**, 360-366; (b) F. Su, S. C. Mathew, G. Lipner, X. Fu, M. Antonietti, S. Blechert and X. Wang, *J. Am. Chem. Soc.* 2010, **132**, 16299-16301; (c) C. Dai and B. Liu, *Energy Environ. Sci.* 2020, **13**, 24-52; (d) V. R. Battula, H. Singh, S. Kumar, I. Bala, S. K. Pal and K. Kailasam, *ACS Catal.* 2018, **8**, 6751-6759.
4. (a) T. Ju, Y.-Q. Zhou, K.-G. Cao, Q. Fu, J.-H. Ye, G.-Q. Sun, X.-F. Liu, L. Chen, L.-L. Liao and D.-G. Yu, *Nat. Catal.* 2021, **4**, 304-311; (b) L. D. Elliott, S. Kayal, M. W. George and K. Booker-Milburn, *J. Am. Chem. Soc.* 2020, **142**, 14947-14956.
5. M. Majek, F. Filace and A. J. v. Wangelin, Beilstein *J. Org. Chem.* 2014, **10**, 981-989.
6. (a) N. D. Bartolo and K. A. Woerpel, *J. Org. Chem.* 2018, **83**, 10197-10206; (b) N. D. Bartolo and K. A. Woerpel, *J. Org. Chem.* 2020, **85**, 7848-7862.
7. S. Su, F.-S. Du and Z.-C. Li, *Org. Biomol. Chem.* 2017, **15**, 8384-8392.
8. (a) R. Englman and J. Jortner, *Molecular Physics* 1970, **18**, 145-164; (b) H. Uoyama, K. Goushi, K. Shizu, H. Nomura and C. Adachi, *Nature* 2012, **492**, 234-238; (c) K. Y. Zhang, Q. Yu, H. Wei, S. Liu, Q. Zhao and W. Huang, *Chem. Rev.* 2018, **118**, 1770-1839.
9. X. Shi, X. Chen, Y. Huang, Z. Liu, B. Zhao, L. Yan, T.-S. Zhang, H. Fu and L. Wang, *Chem. Sci.* 2026, DOI: 10.1039/d5sc06978e.
10. (a) Q. Shi, X. Shi, C. Feng, Y. Wu, N. Zheng, J. Liu, X. Wu, H. Chen, A. Peng, J. Li, L. Jiang, H. Fu, Z. Xie, S. R. Marder, S. B. Blakey and H. Huang, *Angew. Chem. Int. Ed.* 2021, **60**, 2924-2928; (b) L. Ma, S. Wang, Y. Li, Q. Shi, W. Xie, H. Chen, X. Wang, W. Zhu, L. Jiang, R. Chen, Q. Peng and H. Huang, *CCS Chem.* 2022, **4**, 3669-3676.
11. F. Berger, M. B. Plutschack, J. Riegger, W. Yu, S. Speicher, M. Ho, N. Frank and T. Ritter, *Nature* 2019, **567**, 223-228.
12. (a) K. Müller, C. Faeh and F. Diederich, *Science* 2007, **317**, 1881-1886; (b) S. Purser, P. R. Moore, S. Swallow and V. Gouverneur, *Chem. Soc. Rev.* 2008, **37**, 320-330.
13. W. K. Hagmann, *J. Med. Chem.* 2008, **51**, 4359-4369.
14. F. Ye, F. Berger, H. Jia, J. Ford, A. Wortman, J. Börgel, C. Genicot and T. Ritter, *Angew. Chem. Int. Ed.* 2019, **58**, 14615-14619.
15. (a) V. Bhardwaj, D. Gumber, V. Abbot, S. Dhiman and P. Sharma, *RSC Adv.* 2015, **5**, 15233-15266; (b) J. M. Gottesfeld, L. Neely, J. W. Trauger, E. E. Baird and P. B. Dervan, *Nature* 1997, **387**, 202-205.
16. I. H. Jenkins, U. Salzner and P. G. Pickup, *Chem. Mater.* 1996, **8**, 2444-2450.
17. (a) N. Schneider, D. M. Lowe, R. A. Sayle, M. A. Tarselli and G. A. Landrum, *J. Med. Chem.* 2016, **59**, 4385-4402; (b) P. Lloyd-Williams and E. Giralt, *Chem. Soc. Rev.* 2001, **30**, 145-157; (c) H. Xiong, Q. Lin, Y. Lu, D. Zheng, Y. Li, S. Wang, W. Xie, C. Li, X. Zhang, Y. Lin, Z.-X. Wang, Q. Shi, T. J. Marks and H. Huang, *Nat. Mater.* 2024, **23**, 695-702; (d) J. O. Rothbaum, A. Motta, Y. Kratish and T. J. Marks, *J. Am. Chem. Soc.* 2022, **144**, 17086-17096; (e) A. J. Kalin, S. Che, C. Wang, A. U. Mu, E. M. Duka and L. Fang, *Macromolecules* 2020, **53**, 922-928; (f) J. Mei, N. C.

View Article Online
DOI: 10.1039/D6SC01097K

Heston, S. V. Vasilyeva and J. R. Reynolds, *Macromolecules* 2009, **42**, 1482-1487.

18. (a) X. Liang, K. Wen, Q. Shi, B.-B. Zhang, S. Pei, Q. Lin, B. Ma, S. Wang, M. Zhang, X. Li, Z.-X. Wang and H. Huang, *Chem. Eur. J.* 2022, **28**, e202200869; (b) X. Wen, W. Xie, Y. Li, X. Ma, Z. Liu, X. Han, K. Wen, F. Zhang, Y. Lin, Q. Shi, A. Peng and H. Huang, *Angew. Chem. Int. Ed.* 2023, **62**, e202309922; (c) E. Block, *Angew. Chem. Int. Ed.* 1992, **31**, 1135-1178; (d) K. L. Dunbar, D. H. Scharf, A. Litomska and C. Hertweck, *Chem. Rev.* 2017, **117**, 5521-5577; (e) M. Teders, C. Henkel, L. Anhäuser, F. Strieth-Kalthoff, A. Gómez-Suárez, R. Kleinmans, A. Kahnt, A. Rentmeister, D. Guldi and F. Glorius, *Nat. Chem.* 2018, **10**, 981-988.

View Article Online
DOI: 10.1039/D6SC01097K

Data availability

All data needed to evaluate the conclusions in the paper are present in the paper and/or the Supplementary Materials.